Chemical Research in Toxicology

ARTICLE

pubs.acs.org/crt

1,N^2-Etheno-2′-deoxyguanosine Adopts the *syn* Conformation about the Glycosyl Bond When Mismatched with Deoxyadenosine

Ganesh Shanmugam,[†] Ivan D. Kozekov,[†] F. Peter Guengerich,[‡] Carmelo J. Rizzo,[†] and Michael P. Stone*[,†,‡]

[†]Department of Chemistry and [‡]Department of Biochemistry, Vanderbilt Institute of Chemical Biology, Center in Molecular Toxicology, and Vanderbilt-Ingram Cancer Center, Vanderbilt University, Nashville, Tennessee 37235-1822, United States

Supporting Information

ABSTRACT: The oligodeoxynucleotide 5′-CGCATX-GAATCC-3′·5′-GGATTCAATGCG-3′ containing 1,N^2-etheno-2′-deoxyguanosine (1,N^2-εdG) opposite deoxyadenosine (named the 1,N^2-εdG·dA duplex) models the mismatched adenine product associated with error-prone bypass of 1,N^2-εdG by the *Sulfolobus solfataricus* P2 DNA polymerase IV (Dpo4) and by *Escherichia coli* polymerases pol I *exo*$^-$ and pol II *exo*$^-$. At pH 5.2, the T_m of this duplex was increased by 3 °C as compared to the duplex in which the 1,N^2-εdG lesion is opposite dC, and it was increased by 2 °C compared to the duplex in which guanine is opposite dA (the dG·dA duplex). A strong NOE between the 1,N^2-εdG imidazole proton and the anomeric proton of the attached deoxyribose, accompanied by strong NOEs to the minor groove A^{20} H2 proton and the mismatched A^{19} H2 proton from the complementary strand, establish that 1,N^2-εdG rotated about the glycosyl bond from the *anti* to the *syn* conformation. The etheno moiety was placed into the major groove. This resulted in NOEs between the etheno protons and T^5 CH_3. A strong NOE between A^{20} H2 and A^{19} H2 protons established that A^{19}, opposite to 1,N^2-εdG, adopted the *anti* conformation and was directed toward the helix. The downfield shifts of the A^{19} amino protons suggested protonation of dA. Thus, the protonated 1,N^2-εdG·dA base pair was stabilized by hydrogen bonds between 1,N^2-εdG N1 and A^{19} N1H$^+$ and between 1,N^2-εdG O^9 and A^{19} N^6H. The broad imino proton resonances for the 5′- and 3′-flanking bases suggested that both neighboring base pairs were perturbed. The increased stability of the 1,N^2-εdG·dA base pair, compared to that of the 1,N^2-εdG·dC base pair, correlated with the mismatch adenine product observed during the bypass of 1,N^2-εdG by the Dpo4 polymerase, suggesting that stabilization of this mismatch may be significant with regard to the biological processing of 1,N^2-εdG.

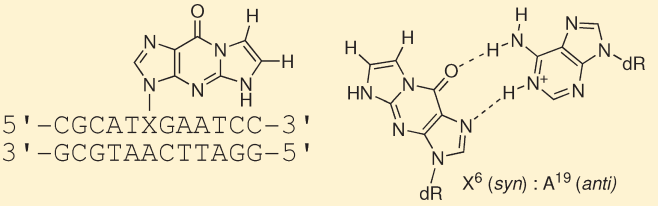

1. INTRODUCTION

Ethenobases[1] arise from the reactions of electrophiles derived from vinyl halides and other vinyl monomers, including chloroacetaldehyde, with dC, dA, and dG in DNA.[2−9] These lesions also arise from endogenous exposures to lipid peroxidation products,[10] particularly 4,5-epoxy-2(*E*)-decanal[11,12] and 4-hydroperoxynonenal.[13] Related etheno adducts from 4-oxo-2(*E*)-nonenal,[14,15] 4-oxohexenal,[16] and 9,12-dioxo-10(*E*)-dodecanoic acid[17] have also been characterized.[15,17] The 1,N^2-ethenodeoxyguanosine (1,N^2-εdG) adduct[18] (Chart 1) is one of two εdG lesions, the other being the N^2,3-εdG adduct. Formation of 1,N^2-εdG proceeds via a Schiff base intermediate involving N^2-dG and the 2-haloacetaldehyde and subsequent nucleophilic attack by N1-dG at the methylene carbon.[19,20] The 1,N^2-εdG lesion has been detected in DNA treated with vinyl chloride metabolites[21] and β-carotene oxidation products.[22] It has been isolated using immunohistochemistry[23] and identified by mass spectrometry in liver DNA of rodents.[24−27]

The 1,N^2-εdG lesion blocks the Watson−Crick face of dG and is anticipated to be mutagenic. Consistent with this expectation, Langouët et al.[28] reported that insertion of bacteriophage M13MB19 site-specifically modified with 1,N^2-εdG into uvrA$^-$ *Escherichia coli* yielded 2% G → A, 0.7% G → T, and 0.1% G → C mutations. In Chinese hamster ovary cells, 1,N^2-εdG induced mutations at levels estimated at 4−8%.[29]

Chart 1. Nucleotide Numbering Scheme of the 1,N^2-εdG·A Modified Duplex (A) and Structure and Numbering Scheme for 1,N^2-εdG, Which Differs from That of dG (B)[a]

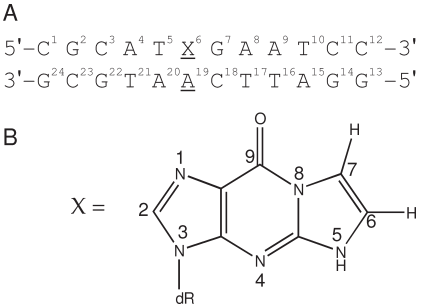

[a]X represents 1,N^2-εdG. The imidazole proton of 1,N^2-εdG is designated as H2, corresponding to the H8 proton in guanine.

Received: February 25, 2011
Published: June 16, 2011

Scheme 1. Potential Mechanisms of the Misincorporation of dATP Opposite 1,N^2-εdG during Error-Prone Trans-Lesion Replication[a]

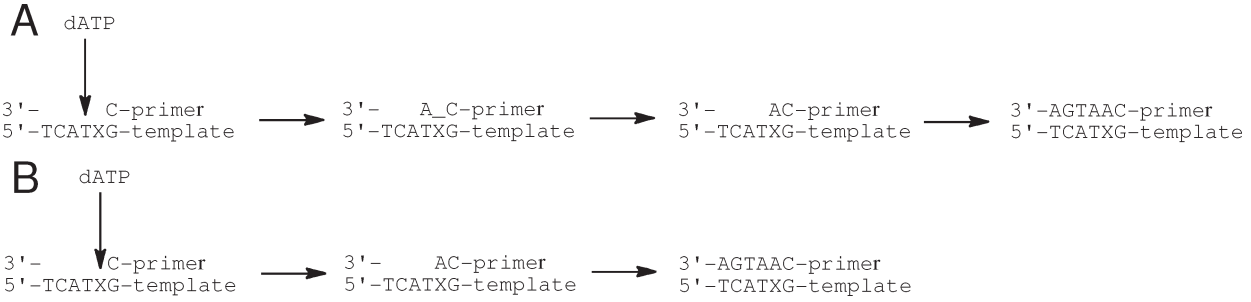

[a] (A) "Type II" mechanism proposed for the misincorporation of dATP by the Dpo4 polymerase. (B) Direct incorporation of dATP opposite the 1,N^2-εdG lesion. X represents the 1,N^2-εdG lesion.

The insertion of 1,N^2-εdG into a 3′-G(1,N^2-εdG)TACT-5′ template and its replication by the *Sulfolobus solfataricus* P2 DNA polymerase IV (Dpo4) was reported by Zang et al.[30] They showed that dATP was preferentially incorporated opposite 1,N^2-εdG. Analyses of binary and ternary complexes with the Dpo4 polymerase[30] suggested that this occurred via the formation of a "Type II" complex at the active site, in which the incoming dATP paired with the 5′-neighboring T of the template strand, as opposed to 1,N^2-εdG.[31] Relaxation of the "Type II" complex followed by extension presumably led to the full length 5′-AATGA-3′ product,[30] which if not recognized by mismatch repair, would ultimately yield a G → T transversion (Scheme 1).

Duplexes containing 1,N^2-εdG opposite dC were structurally characterized.[32−34] When 1,N^2-εdG was placed opposite dC in the 3′-G(1,N^2-εdG)T-5′ sequence, it existed as an equilibrium mixture of *syn* and *anti* conformers about the glycosyl bond.[33,34] In the *anti* conformation 1,N^2-εdG was inserted into the duplex but was shifted toward the minor groove as compared to dG in a Watson−Crick C·G base pair. The complementary cytosine was displaced.[34] Protonation of dC allowed Hoogsteen pairing when 1,N^2-εdG was in the *syn* conformation and placed the etheno moiety into the major groove.[33] In the 3′-G(1,N^2-εdG)T-5′ sequence, a second conformational equilibrium was observed, in which the modified base pair and its 3′-neighboring G·C base pair formed tandem Hoogsteen pairs. Zaliznyak et al.[32] also reported a *anti*/*syn* equilibrium for 1,N^2-εdG in the 3′-C(1,N^2-εdG)C-5′ sequence when placed complementary to dC.

Presently, we have examined 1,N^2-εdG opposite dA in 5′-d(CGCATXGAATCC)-3′·5′-d(GGATTCAATGCG)-3′ (X = 1,N^2-εdG) containing the 3′-G(1,N^2-εdG)TAC-5′ template.[30] This is referred to as the 1,N^2-εdG·dA duplex (Chart 1). It models the putative situation following incorporation of dATP opposite the template 5′-neighbor T, as opposed to 1,N^2-εdG,[30] followed by relaxation of the "Type II" complex[31] and extension, which would result in the mis-insertion of dATP opposite 1,N^2-εdG. The data reveal a pH-dependent conformational transition of 1,N^2-εdG. At pH 5.2, the 1,N^2-εdG·dA base pair exhibits a higher T_m than does the 1,N^2-εdG·dC base pair. Moreover, the 1,N^2-εdG·dA base pair is more stable than is the dG·dA base pair. The 1,N^2-εdG base rotates about the glycosyl bond from the *anti* to the *syn* conformation at pH 5.2. This places the 1,N^2-εdG etheno moiety into the major groove. The chemical shifts of the N^6-dA amino protons suggest that it undergoes protonation at N1, forming a 1,N^2-εdG·dA base pair stabilized by two hydrogen bonds. The increased stability of 1,N^2-εdG opposite dA correlates with the 5′-AATGA-3′ primer product observed during the bypass of 1,N^2-εdG by the Dpo4 polymerase.[30] The stability of this mismatched dA may impact the biological processing of 1,N^2-εdG.

2. MATERIALS AND METHODS

2.1. Sample Preparation. The oligodeoxynucleotides 5′-d(CGCATGGAATCC)-3′ and 5′-d(GGATTCCATGCG)-3′ were synthesized and purified by anion-exchange chromatography by the Midland Certified Reagent Company (Midland, TX). The 1,N^2-εdG containing oligodeoxynucleotide 5′-d(CGCATXGAATCC)-3′ (X = 1,N^2-εdG) was synthesized, purified, and characterized as previously described.[34,35] Oligodeoxynucleotide concentrations were determined from UV absorbance using calculated extension coefficients at 260 nm.[36]

2.2. Thermal Melting (T_m) Studies. Experiments were conducted using a Cary 100 Bio UV−vis spectrophotometer (Varian Associates, Palo Alto, CA). The 1,N^2-εdG-modified strand and mismatched dA-containing complementary strand were mixed in a 1:1 molar ratio, in aqueous solution, at room temperature. The duplex was eluted from DNA grade Biogel hydroxylapatite (Bio-Rad Laboratories, Richmond, CA) to remove excess single strand, using a gradient from 10 to 100 mM NaH_2PO_4 buffer at pH 7.0. It was desalted using Sephadex G-25. Samples contained 0.3 A_{260} units of duplex in 1 mL of buffer containing 10 mM NaH_2PO_4, 100 mM NaCl, and 5 μM EDTA (pH 5.2) in a 1.0 cm cuvette. The UV absorbance at 260 nm was recorded at 1 min intervals with a temperature gradient of 2.5 °C/min. The temperature was cycled between 15 and 70 °C. The T_m value was determined from the first derivative of the melting curves.

2.3. NMR. Samples were dissolved to a duplex concentration of 0.5 mM in 500 μL of buffer containing 10 mM NaH_2PO_4, 100 mM NaCl, and 5 μM Na_2EDTA (pH 5.2; uncorrected for deuterium isotope effects). For the observation of nonexchangeable protons, samples were exchanged with D_2O and suspended in 500 μL of 99.99% D_2O. For the observation of exchangeable protons, samples were dissolved to a concentration of 0.5 mM in 500 μL of buffer containing 10 mM NaH_2PO_4, 100 mM NaCl, and 5 μM Na_2EDTA (pH 5.2) 9:1 H_2O/D_2O (v/v). The pH was adjusted by titration with DCl. Chemical shifts of the proton resonances were referenced to water. NMR spectra were recorded at 600 MHz. For each t_1 increment of ^{1}H NOESY experiments in D_2O, 32 scans were averaged with presaturation of the HDO resonance. Spectra were recorded consecutively using TPPI phase cycling with mixing times of 70, 150, 200, and 250 ms. These were recorded with 2048 complex points in the acquisition dimension and 1024 real data points in the indirect dimension covering 9615.385 Hz.

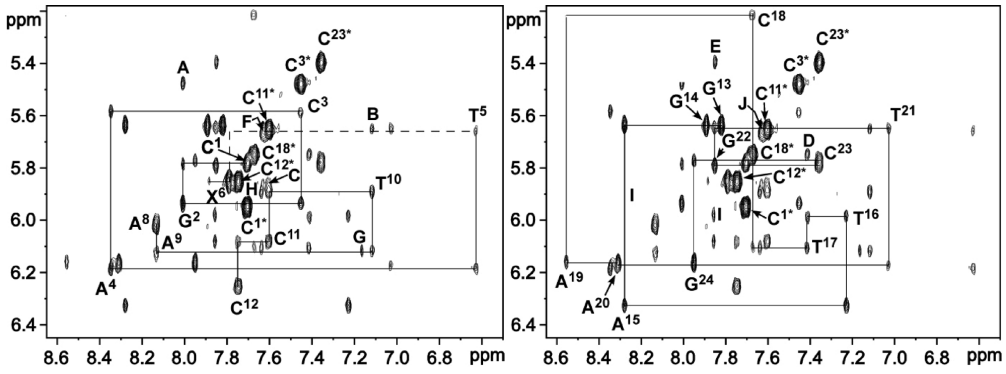

Figure 1. Expansion of the NOESY spectrum, showing the sequential assignment of NOEs between purine H8/pyrimidine H6 and the deoxyribose H1′ protons and the 3′-neighbor deoxyribose H1′ protons, for the 1,N^2-εdG·dA duplex. In the 1,N^2-εdG-modified strand (left panel), interruptions are observed at X^6, where the T^5 H1′ → X^6 H2 and G^7 H8 → G^7 H1′ NOEs are missing. In the complementary strand (right panel), no interruptions are observed in the sequential NOEs. A weak NOE is observed between C^{18} H1′ and A^{19} H8 at a lower threshold level. Labeled peaks: A, G^2 H8 → C^3 H5; B, T^{10} H6 → C^{11} H5; C, C^{11} H6 → C^{12} H5; D, T^{17} H6 → C^{18} H5; E, G^{22} H8 → C^{23} H5; F, A^4 H2 → T^5 H1′; G, A^8 H2 → A^9 H1′; H, A^9 H2 → T^{10} H1′; I, A^{15} H2 → T^{16} H1′; and J, A^{20} H2 → T^{21} H1′. The spectrum was recorded at 250 ms mixing time at 25 °C.

The relaxation delay was 1.5 s. The data in the d_2 dimension were zero-filled to give a matrix of 2K × 2K real points. NOESY spectra for the observation of exchangeable protons were recorded in 9:1 H_2O/D_2O (v/v), using the Watergate pulse sequence[37] for water suppression. The spectra, consisting of 128 transients, were obtained with a cryogenic probe using States-TPPI phase cycling with a mixing time of 250 ms. A squared sine-bell with 72° shift apodization was applied in the d_1 dimension while cosine-squared bell apodization was applied in the d_2 dimension. A total of 1536 real data points in the d_1 dimension and 512 points in the d_2 dimension were acquired. Chemical shifts of proton resonances were referenced to water. NMR data were processed on Silicon Graphics Octane workstations and assigned using FELIX2000 (Accelrys, San Diego, CA).

3. RESULTS

3.1. Characterization of the 1,N^2-εdG·dA Duplex. The 1,N^2-εdG-containing oligodeoxynucleotide was characterized by mass spectrometry and enzymatic digestion as previously described.[33] The 1,N^2-εdG·dA duplex was also analyzed using CGE and C-18 HPLC. Both the techniques yielded two peaks, of equal intensities, corresponding to the 1,N^2-εdG-modified and complementary strands.

3.2. Stability of the 1,N^2-εdG·A Duplex. When dG was mismatched with dA (dG·dA), the 5′-CGCATGGAATCC-3′·5′-GGATTCAATGCG-3′ duplex showed a T_m that was 12 °C less (~41 °C) than that of the corresponding duplex containing the dG·dC base pair, which was 53 °C. Introduction of 1,N^2-εdG opposite dA (1,N^2-εdG·dA) showed a modest increase in T_m, from 41 to 43 °C, as compared to that of the dG·dA duplex. But the T_m of the duplex containing the 1,N^2-εdG·dC base pair was 40 °C. Thus, the 1,N^2-εdG·dA duplex was more stable than the 1,N^2-εdG·dC duplex and less stable when compared to the dG·dC duplex under similar conditions.

3.3. NMR of the 1,N^2-εdG·dA Duplex at pH 5.2. The ^{1}H NMR spectra of the duplex were dependent upon pH. At pH 5.2 and 7 °C, the spectra exhibited reasonably sharp ^{1}H resonances, albeit with spectral broadening proximate to X^6. Six COSY peaks accounted for all cytosine H5−H6 scalar couplings of the duplex. Accordingly, characterization was carried out at pH 5.2 and at 7 °C. The NMR spectra were not of sufficient quality to enable the measurement of distance and torsion angle restraints required to refine the solution structure of the 1,N^2-εdG·dA duplex.

3.3.1. Nonexchangeable Protons. The nonexchangeable DNA protons were assigned using standard protocols.[38,39] An expanded plot of NOE sequential connectivity between the nucleobase and the deoxyribose H1′ protons is shown in Figure 1. Only one set of NOE resonances was observed for 1,N^2-εdG and other nucleotides. The anticipated sequential NOE connectivity between base aromatic and deoxyribose anomeric protons was interrupted in both the modified and complementary strands. In the modified strand, the A^4 H1′ → T^5 H6 and T^5 H6 → T^5 H1′ NOEs were weak. The T^5 H1′ → X^6 H2 NOE was missing (Figure 1A; note that the X^6 imidazole proton is designated as H2). The intensity of the X^6 H1′ → X^6 H2 NOE was exceptionally strong. This NOE remained present in the spectrum recorded at 70 ms mixing time, characteristic of the *syn* conformation about the glycosyl bond (Figure 2). The X^6 H1′ → G^7 H8 NOE was weak. The G^7 H8 → G^7 H1′ and G^7 H1′ → A^8 H1′ NOEs were missing (Figure 1, left panel). Proceeding in the 3′-direction from the A^8 H8 → A^8 H1′ NOE, the NOESY connectivity continued uninterrupted to the 3′ terminus of the modified strand. In the complementary strand, the T^{17} H1′ → C^{18} H8 and C^{18} H8 → C^{18} H1′ NOEs were broad and overlapped (Figure 1, right panel). The sequential connectivity was interrupted between C^{18} H1′ and A^{19} H8. The A^{19} H1′ and A^{20} H1′ resonances overlapped. As a result, the intensities of the A^{19} H1′ → A^{20} H8 NOEs could not be determined with certainty. Proceeding in the 3′-direction from the A^{20} H8 → A^{20} H1′ NOE, the NOE connectivity continued uninterrupted to the 3′ terminus of the modified strand (Figure 1, right panel).

Characteristic NOEs for B-type DNA were identified, except between T^5 and A^8 and between the C^{18} and A^{20} nucleotides. For example, the sequential NOEs between aromatic base proton and 3′-neighbor cytosine H5 protons, G^2 H8 → C^3 H5, T^{10} H6 → C^{11} H5, C^{11} H6 → C^{12} H5, T^{17} H6 → C^{18} H5, and G^{22} H8 → C^{23} H5 (peaks A, B, and C, Figure 1 (left panel) and D and E, Figure 1 (right panel), respectively), and NOEs between adenine H2 proton and 3′-neighbor H1′ protons, A^4 H2 → T^5 H1′, A^8 H2 → A^9 H1′, A^9 H2 → T^{10} H1′, A^{15} H2 → T^{16} H1′, and A^{20} H2 → T^{21} H1′ (peaks F, G, and H Figure 1 (left panel), and I

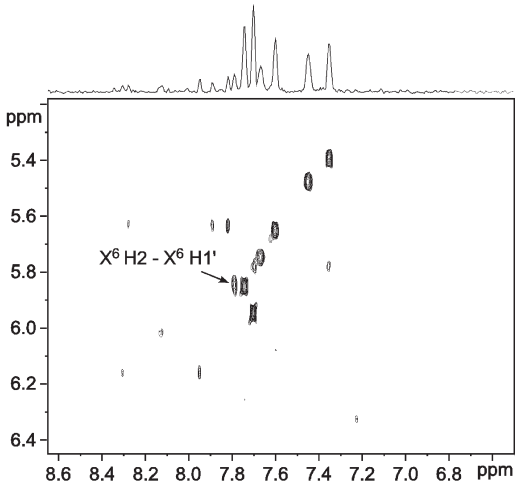

Figure 2. Expansion of the NOESY spectrum, collected at 70 ms mixing time, showing the NOE connectivity between X^6 H2 and X^6 H1′ protons.

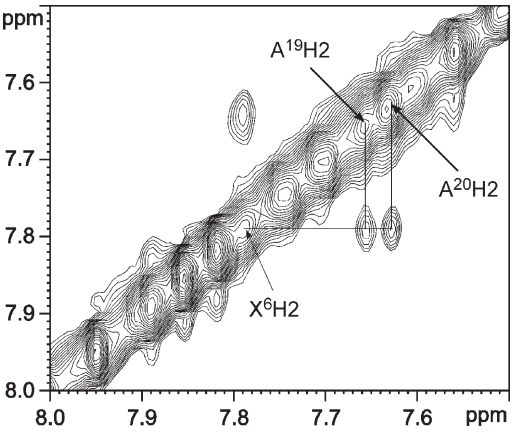

Figure 3. Expansion of the NOESY spectrum collected at 250 ms mixing time showing the two additional cross-peaks that were assigned to X^6 H2 → A^{19} H2 and X^6 H2 → A^{20} H2 NOEs. The contour threshold level of this spectrum was increased 0.5×, compared to Figure 2, to make the cross-peaks stand out.

and J, Figure 1 (right panel), respectively), were observed. The sequential A^{19} H2 → A^{20} H1′ NOE was weak (not observed at the contour level plotted in Figure 1). Similarly, all intranucleotide NOEs between adenine H2 and deoxyribose H1′ protons, A^4 H2 → A^4 H1′, A^8 H2 → A^8 H1′, A^9 H2 → A^9 H1′, and A^{15} H2 → A^{15} H1′, were observed except for A^{20} H2 → A^{20} H1′, which is the flanking base to the adduct. The A^{19} H2 → A^{19} H1′ NOE overlapped with A^{19} H2 → A^{20} H1′ NOE (Figure 1, right panel). The complete resonance assignment of nonexchangeable protons is tabulated in Table S1 of the Supporting Information.

The assignments of the adenine H2 resonances were based on the assignment of NOEs between the adenine H2 and the H1′ of the attached deoxyribose and H1′ of the 3′-neighbor deoxyribose. Two additional strong NOEs were observed, involving 5′ → 3′ NOEs between aromatic base protons of purines and pyrimidines (Figure 3). These were assigned to X^6 H2 → A^{20} H2 and X^6 H2 → A^{19} H2 protons (Figure 3).

3.3.2. Exchangeable Protons. The spectrum of the imino proton resonance region is shown in Figure 4A. Five resonances for thymine imino protons, T^5 N3H, T^{10} N3H, T^{16} N3H, T^{17} N3H, and T^{21} N3H, and four for guanine imino protons, G^2 N1H, G^7 N1H, G^{14} N1H, and G^{22} N1H, were observed between 13.8 and 13.2 ppm and between 13.1 and 11.5 ppm, respectively. Note that 1,N^2-εdG lacks an imino proton. The G^7 N1H and T^5 N3H resonances were broad. The imino protons of the two terminal base pairs were not observed, presumably due to exchange with water. The imino protons were assigned from NOEs between adjacent base pairs and between their corresponding base-paired N^4-dC amino and H2-dA protons.[40] The assignment of all H2-dA protons allowed for the identification of the dA·dT base pairs (Figure 4B and C). Similarly, the assignment of all N^4-dC amino protons, observed from their intranucleotide NOEs to the H5-dC protons, detected in the 250 ms mixing time spectrum, allowed for the identification of the dG·dC base pairs, except C^{18} (Figure 4B). The G^7 N1H assignment was supported by the finding of the 1,N^2-εdG (*syn*)·dC (*anti*) base pair in the same 5′-TXG-3′ sequence at pH 5.2. The T^5 N3H protons showed two additional NOE cross-peaks between them (Figure 4C), which were attributed to exchange peaks arising between multiple conformers of T^5. One exchange resonance was separated

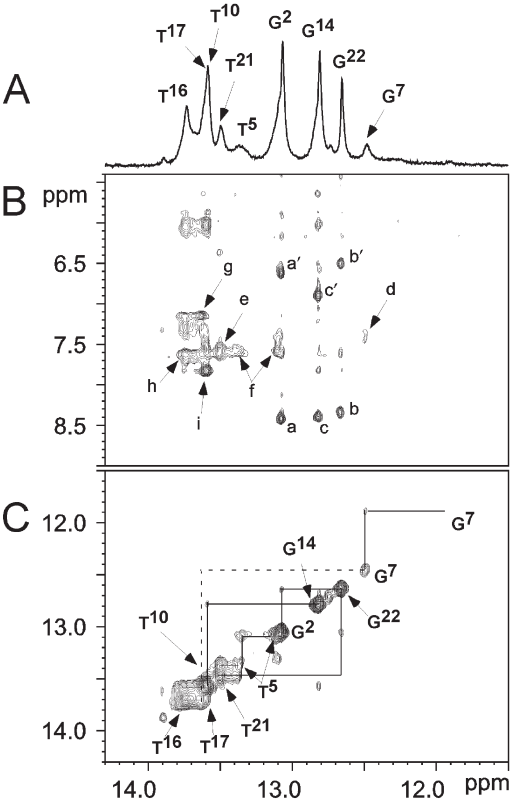

Figure 4. (A) Imino proton region of the NMR spectrum recorded in 9:1 H_2O:D_2O at 5 °C. (B) An expanded NOESY spectrum showing the sequential NOEs from the imino protons to the cytosine amino protons and adenine H2 protons. Labeled NOEs are a,a′, G^2 N1H → C^{23} N^4H, h/n); b,b′, G^{22} N1H → C^3 N^4H, h/n; c,c′, G^{14} N1H → C^{11} N^4H, h/n; d, G^7 N1H → C^{18} N^4H, h (or) n; e, T^{21} N3H → A^4 H2; f, T^5 N3H → A^{20} H2; g, T^{17} N3H → A^8 H2; h, T^{16} N3H → A^9 H2; i, T^{10} N3H → A^{15} H2. (C) An expanded NOESY spectrum showing the sequential NOEs between the imino protons. The data were collected at 600 MHz at 250 ms mixing time and at 5 °C.

and the other resonance, observed within the broad resonance of G^7 N1H, was close to the diagonal (Figure 4C). The sequential NOE

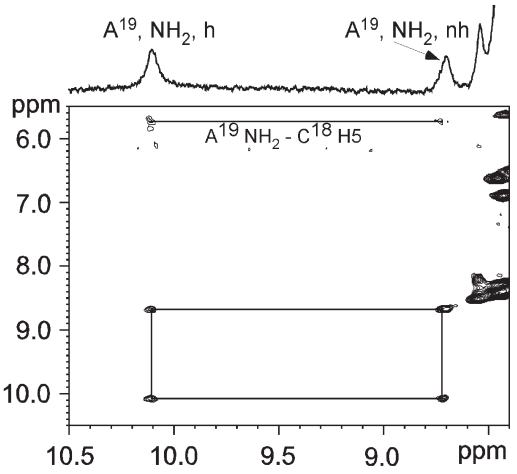

Figure 5. Expanded region of the NOESY spectrum showing the downfield shifts of A^{19} (complementary to X^6) amino proton resonances compared to other adenine amino protons in the duplex and an NOE between the corresponding amino protons. These resonances are observed at 8.66 and 10.07 ppm. The downfield chemical shifts of the A^{19} amino protons are characteristic of pairing at $X^6 \cdot A^{19}$ base pairs. The spectrum was recorded in 9:1 H_2O:D_2O at 5 °C.

cross-peaks were observed for base pairs $G^2 \cdot C^{23}$, $C^3 \cdot G^{22}$, $A^4 \cdot T^{21}$ and $T^5 \cdot A^{20}$, which are located in the 5′-direction from the 1,N^2-εdG adduct (Figure 4C). Likewise, sequential NOE connectivity was observed between base pairs $A^8 \cdot T^{17}$, $A^9 \cdot T^{16}$, $T^{10} \cdot A^{15}$, and $C^{11} \cdot G^{14}$, which are located in the 3′-direction from the 1,N^2-εdG adduct. Thus, the sequential NOE connectivity was interrupted from $T^5 \cdot A^{20}$ to $A^8 \cdot T^{17}$ base pairs. The complete set of imino proton assignments is tabulated in Table S2 of the Supporting Information.

Figure 5 shows two additional resonances at 8.7 and 10.1 ppm, which were assigned to the amino protons of protonated A^{19}, complementary to 1,N^2-εdG, at pH 5.2. These disappeared at pH 7.0. The resonance at 10.1 ppm was assigned to the A^{19} hydrogen-bonded amino proton, while the resonance at 8.7 ppm was assigned to the A^{19} non-hydrogen-bonded amino proton. A NOE was observed between these two amino protons, and weak NOEs were identified between the amino protons and its 5′-neighbor C^{18} H5 proton (Figure 5). No other NOEs were observed for the A^{19} amino protons, presumably due to the disorder of the neighboring base pairs.

3.3.3. Etheno Protons. A tile plot of the NOESY spectrum recorded at 250 ms mixing time (Figure 6) shows the assignment of the etheno protons and also NOEs between the etheno protons and nonexchangeable DNA protons. The H6 and H7 etheno proton resonances were identified from spectra recorded at 70 and 250 ms, in which similar intensity NOEs were observed between 7.26 and 7.32 ppm (Figure 6, peak a). Similar chemical shifts for the etheno protons were observed for 1,N^2-εdG (*syn*)·C (*anti*) base pairs inserted into the same duplex at pH 5.2 (Table 1). In the latter case, the etheno H6 and H7 resonances were degenerate at 7.33 ppm. Five NOEs were observed between the etheno and DNA protons and all involved NOEs with 5′-neighbor T^5. Strong NOEs were observed between X^6 H6/H7 and T^5 CH_3 protons (Figure 6, peak c and f). Three weak NOEs were assigned to X^6 H7/H6 and the T^5 H6 and H2′ protons, in which one of the NOEs X^6 H7/H6 → T^5 H2′ was overlapped with X^6 H7/H6 → T^5 CH_3 (Figure 6, peak e and f).

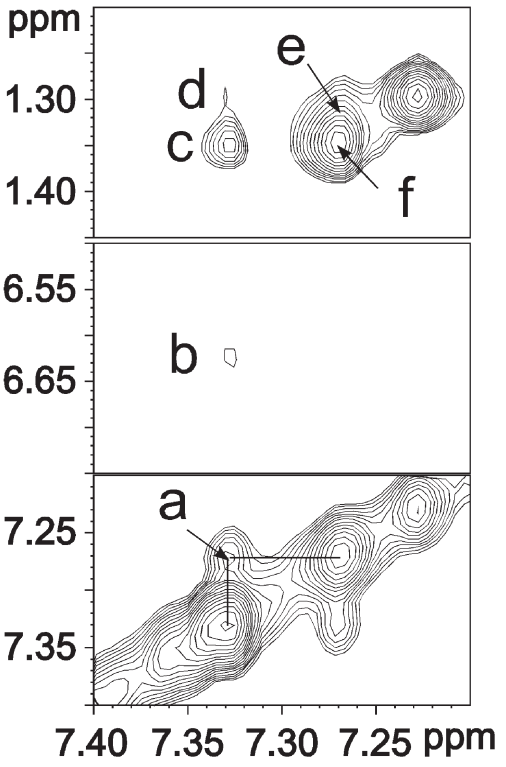

Figure 6. Expanded NOESY spectrum (tile plot) showing the assignment of the H6 and H7 etheno protons and NOEs between the etheno and DNA protons. The spectrum was recorded at 7 °C with 250 ms mixing time. Cross-peaks: a, X^6 H7 → X^6 H6; b, X^6 H7/H6 → T^5 H6; c, X^6 H7/H6 → T^5 CH_3; d, X^6 H7/H6 → T^5 H2′; e, X^6 H7/H6 → T^5 H2′; f, X^6 H7/H6 → T^5 CH_3. The contour threshold level of the bottom panel was increased by 0.3×, compared to other panels, to show the NOE cross-peak X^6 H7 → X^6 H6 (peak a) more clearly.

3.4. Chemical Shifts of Etheno Protons. Table 1 compiles chemical shifts of the etheno protons in the 1,N^2-εdG·dA duplex at pH 5.2 in comparison with a series of related duplexes. The chemical shifts of the etheno protons in the 1,N^2-εdG·dA duplex were similar to those in the 1,N^2-εdG·dC duplex. The resonances of the etheno protons shifted downfield compared to the 1,N^2-εdG·C and 1,N^2-εdG-1BD duplexes at pH 8.6 and 7.0, respectively, where 1,N^2-εdG adopted the *anti* conformation and was accommodated in an intrahelical orientation.

4. DISCUSSION

The 1,N^2-εdG adduct prevents Watson−Crick hydrogen bonding. Not surprisingly, the replicative polymerase pol δ is blocked by 1,N^2-εdG.[41] 1,N^2-εdG is mutagenic in *E. coli*, inducing 0.7% G → T transversions,[28] and in mammalian cells.[29] Zang et al.[30] characterized the bypass of 1,N^2-εdG using the Dpo4 polymerase and showed that it preferentially incorporates dATP when challenged by the template sequence 3′-G(1,N^2-εdG)TAC-5′; a one-base deletion was also observed. Zang et al.[30] proposed that these outcomes occur via the formation of a "Type II" complex at the active site, in which the incoming dATP pairs with the template 5′-neighbor T, as opposed to 1,N^2-εdG.[31] Relaxation and further extension leads to a duplex containing the 1,N^2-edG·A mismatch,[30] which if not corrected, would ultimately yield a G → T transversion. If relaxation of the "Type II" complex does not occur, further

Table 1. Chemical Shift Comparison of the Etheno Protons of 1,N^2-εdG in Different Oligodeoxynucleotide Duplexes

	1,N^2-εdG·C Duplex		1,N^2-εdG-1BD duplex[c]	1,N^2-εdG·A duplex
protons	1,N^2-εdG(*anti*)·C(*anti*) (pH 8.6)[a]	1,N^2-εdG(*syn*)·C(*anti*) (pH 5.2)[b]	1,N^2-εdG(*anti*) (pH 7.0)	1,N^2-εdG(*syn*)·A(*anti*) (pH 5.2)
H6	6.21	7.33	5.55	7.26[d]
H7	6.54	7.33	5.84	7.32[d]

[a] Chemical shift values as reported.[34] [b] Chemical shift values as reported.[33] [c] Chemical shift values as reported.[47] [d] Resonances were not assigned unequivocally.

extension yields the −1 deletion product.[30] It was thus of interest to examine the 1,N^2-εdG·A mismatch, the putative intermediate that would lead to G → T transversions when 1,N^2-εdG is bypassed by the Dpo4 polymerase.[30]

4.1. Stability of the 1,N^2-εdG·A Duplex. At pH 5.2, mispairing of dA opposite 1,N^2-εdG increased the T_m as compared to the 1,N^2-εdG·C base pair (43 vs 40 °C). Moreover, the T_m of the 1,N^2-εdG·A duplex is 2 °C higher than that of the dG·dA duplex. These data correlate with the ability of the Dpo4 polymerase to incorporate dATP opposite 1,N^2-εdG in the 3′-G(1,N^2-εdG)TAC-5′ template, leading either to a 5′-CAATG-3′ primer extension product or to the 5′-CATG-3′ deletion product.[30] Both outcomes are consistent with the structural data that suggests that this polymerase favors using the 5′-neighbor thymine (underlined) to incorporate dATP via a Type II complex.[31] The overall misinsertion of dATP[30] may result from relaxation of the initially formed Type II complex to the 1,N^2-εdG·A mismatch followed by extension. Incorporation of dATP also predominates during the bypass of 1,N^2-εdG by *E. coli* polymerases pol I *exo*$^-$ and pol II *exo*$^-$ using a 5′-TXT-3′ damaged template, also containing the template 5′-neighbor T.[42] Other polymerases, however, may use different mechanisms to bypass the lesion. Human polymerase η preferentially incorporates dGTP, irrespective of the identity of the base 5′ to 1,N^2-εdG in the template.[41] The human polymerases ι and κ show similar rates of incorporation of dTTP and dCTP.[41]

4.2. Glycosyl Torsion Angle of 1,N^2-εdG at pH 5.2. When 1,N^2-εdG is mismatched with dA in the 5′-TXG-3′ sequence, the NMR spectrum is dependent upon pH, suggesting that 1,N^2-εdG equilibrates between conformations, similar to the 1,N^2-εdG·dC base pair.[32−34] At pH 5.2, one conformation predominates, and 1,N^2-εdG adopts the *syn* conformation about the glycosyl bond. The strong X^6 H2 → X^6 H1′ NOE and the observation that it remains present at 70 ms NOE mixing time provides evidence for the *syn* conformation. This is corroborated by the failure to observe a NOE between the X^6 H2 proton and the 5′-neighbor H1′ proton, which would be consistent with the increase in distance between those protons. The *syn* conformation of the glycosyl bond also places the X^6 N5 amino proton (Chart 1) in the major groove and exposed to water, which is consistent with the failure to observe it. Furthermore, in the complementary strand, both the A^{19} and A^{20} H2 protons provide markers for monitoring the conformational change from the X^6(*anti*)·A^{19}(*anti*) alignment to the X^6(*syn*)·A^{19}(*anti*) alignment. The appearance of strong NOEs between X^6 H2 and the A^{19} and A^{20} H2 protons is consistent with the *syn* and the *anti* conformations of 1,N^2-εdG and the mismatched dA, respectively (Figure 3). The etheno protons also provide markers for monitoring the conformational change from the *anti* to the *syn* conformations. The etheno proton chemical shifts remain unaltered compared to when 1,N^2-εdG is placed opposite dC at pH 5.2. In that case,

Chart 2. X^6·A^{19} Base Pair Showing the Two Hydrogen Bonds between N1 of 1,N^2-εdG and N1 of A^{19} and between O^9 of 1,N^2-εdG and N^6 of A^{19} Bases[a]

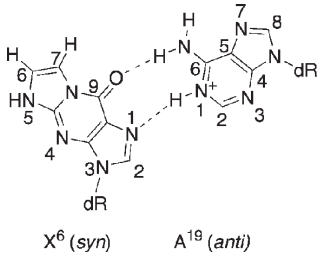

[a] See Chart 1 for modified numbering for 1,N^2-εdG.

1,N^2-εdG adopted the *syn* conformation and is placed into the major groove.[33] At pH 5.2, the X^6 H6 and H7 resonances shift downfield compared to when 1,N^2-εdG is placed opposite dC at pH 8.6 (Table 1). In the latter instance, 1,N^2-εdG adopts the *anti* conformation and is inserted into the duplex.[34] In the *anti* conformation, 1,N^2-εdG shifts toward the minor groove, reducing stacking interactions experienced by the etheno moiety, whereas in the *syn* conformation, 1,N^2-εdG shifts into the major groove, and the etheno moiety is not stacked into the helix, thus explaining the downfield shifts of the etheno proton resonances. Strong NOEs between the etheno protons and the T^5 CH_3 protons (Figure 6) suggest that the etheno moiety orients into the major groove, placing the X^6 H2 proton into the minor groove. The upfield shift of T^5 H6 (Figure 1, left panel) and H2′ (Table S1 in the Supporting Information), compared to other thymine H6 and H2′ protons, correlates with the major groove placement of the etheno moiety. This is attributed to the shielding of 1,N^2-εG in the major groove orientation. The absence of additional NOEs between 1,N^2-εdG etheno protons and DNA protons further confirms the placement of the 1,N^2-εdG etheno protons in the major groove. The *syn* orientation facilitates protonation of A^{19} N3, allowing the formation of the 1,N^2-εdG·A base pair stabilized by Hoogsteen-like hydrogen bonds between 1,N^2-εdG N1 and A^{19} N1H$^+$ and between 1,N^2-εdG O^9 and A^{19} N^6H (Chart 2). The broadening of A^{19} amino proton resonances suggests that these protons undergo facile exchange with water. The weak NOE between G^7 N1H and C^{18} amino protons suggested that the Watson−Crick hydrogen bonding at the 3′-neighbor G^7·C^{18} base pair was intact (Figure 4 B). This was consistent with the broadening of G^7 N1H imino proton resonance (Figure 4A). An additional NOE between the G^7 N1H imino proton at 12.4 ppm and a proton resonating at 11.9 ppm was observed (Figure 4C). This might be attributed to a second conformational equilibrium allowing the formation of a Hoogsteen pair at the 3′-neighbor base pair G^7·C^{18}. A similar equilibrium at the 3′-neighor base pair was observed for the

duplex containing the PdG·dC base pair.[43] However, the broadening of G^7 N1H imino proton resonance suggested that the G^7·C^{18} base pair equilibrated between Watson−Crick and the Hoogsteen pairing, favoring the Watson−Crick pair over the Hoogsteen pair at pH 5.2. Similar downfield-shifted resonances were observed for protonated adenine when dA was mismatched with the *trans*-4-hydroxynonenal (HNE)-derived (6*S*,8*R*,11*S*) 1,N^2-dG adduct[44] in which the HNE-derived 1,N^2-dG adduct adopted the *syn* conformation, and the HNE moiety was in the major groove.

4.3. Flanking Base Pairs. The perturbation induced by the insertion of the 1,N^2-εdG adduct opposite dA extends to its neighboring base pairs. Both 5′-neighbor T^5·A^{20} and 3′-neighbor G^7·C^{18} base pairs show broadening of the imino proton resonances upon insertion of the 1,N^2-εdG·dA pair into the 5′-TXG-3′ sequence. The broad G^7 N1H and T^5 N3H imino proton resonances suggest that these protons are in more rapid exchange with water (Figure 4A). This is also consistent with the weak NOEs between the G^7 N1H imino proton and C^{18} amino protons, and the T^5 N3H imino and A^{20} H2 protons (Figure 4B) and the failure to observe the X^6 H2 → T^5 N1H and X^6 H2 → G^7 N1H NOEs. The weak NOE between the T^5 H6 and T^5 H1′ protons, a missing NOE between the G^7 H6 and G^7 H1′ protons, and a weak NOE between the X^6 H1′ and G^7 H8 protons are also consistent with the perturbation of the flanking nucleotides. This correlates with the thermal melting data in which the 1,N^2-εdG·dA duplex exhibits a 10° drop in T_m as compared to the dG·dC duplex under similar conditions, but significantly, it remains more stable than the 1,N^2-εdG·dC duplex. Since the flanking base pairs remain disordered, a high-resolution structure determination is not possible for this duplex in this sequence context.

4.4. Comparisons with 1,N^2-Propano-2′-deoxyguanosine (PdG) Mismatched with dA. PdG provides an interesting comparison to the 1,N^2-εdG adduct. Duplexes containing PdG·dA base pairs have been characterized.[45,46] The 1,N^2-εdG·dA base pair shows similarities to the PdG·dA base pair. For both, the damaged nucleotide exhibits a transition from the *anti* to the *syn* conformation about the glycosyl bond. The etheno or propano moieties of 1,N^2-εdG and PdG, respectively, are placed into the major groove. In both cases, the protonation of the complementary dA allows stabilization of 1,N^2-εdG·dA or PdG·dA base pairs by two hydrogen bonds (Chart 2). The etheno or propano proton resonances, shift downfield, compared to their resonances when these lesions adopt the *anti* conformation, and their chemical shifts as compared to single strands or mononucleotides, consistent with deshielding from neighboring base pairs and the accommodation of 1,N^2-εdG and PdG in extrahelical orientations.

4.5. Mechanistic Implications. The stability of the 1,N^2-εdG·A mismatch as compared to that of the 1,N^2-εdG·C pair may be significant with regard to the biological processing of 1,N^2-εdG. This mismatch represents an intermediate in several potential mechanisms of error-prone replication bypass. A mechanism proposed by Zang et al.[30] suggests the formation of a "Type II" complex at the Dpo4 polymerase active site, in which the incoming dATP first pairs with the 5′-neighboring template T, as opposed to 1,N^2-εdG (Scheme 1). Relaxation of the "Type II" complex to form the 1,N^2-εdG·A mismatch followed by extension leads to the full length 5′-AATGA-3′ product (Scheme 1), which if not recognized by mismatch repair, would ultimately yield a G → T transversion. Alternatively, if the "Type II" complex does not relax to form the 1,N^2-εdG·A mismatch, further extension would lead to a −1 frameshift event. The duplex containing 1,N^2-εdG opposite a one-base deletion has also been examined, and it also exhibits increased stability but adopts the *anti* conformation of the 1,N^2-εdG glycosyl angle at neutral pH,[47] compared to the duplex containing 1,N^2-εdG·C base pair[33,34] in which 1,N^2-εdG exists in equilibrium between the *syn* and the *anti* conformations. This may correlate with −1 base deletions when 1,N^2-εdG is bypassed by the Dpo4 polymerase.[30] Another possible mechanism for replication bypass involves direct misincorporation of dATP opposite 1,N^2-εdG, followed by extension (Scheme 1). In any event, while protonation at N1 dA and formation of the protonated 1,N^2-εdG·A mismatch with dA in the *syn* conformation about the glycosyl bond will decrease at physiological pH, it is anticipated that a small population of the protonated 1,N^2-εdG·A mismatch would remain, consistent with the observation of 0.7% G → T transversions in *E. coli*.[28]

5. CONCLUSIONS

When mismatched with dA in the 5′-TXG-3′ sequence at pH 5.2, 1,N^2-εdG rotates from the *anti* to the *syn* conformation about the glycosyl bond, similar to 1,N^2-εdG opposite dC.[32,33] While conformational exchange precludes detailed structural refinement, a population of the *syn* conformation seems likely to be present at neutral pH. The duplex containing the 1,N^2-εdG·A mismatch exhibits greater stability as compared to the 1,N^2-εdG·C pair. This may, in part, explain the misincorporation of dATP by the Dpo4 polymerase during error-prone bypass replication.[30] It will be of interest to determine whether the 1,N^2-εdG (*syn*)·A (*anti*) alignment also exists in the primer-template containing 1,N^2-εdG opposite dA in complex with Y-family DNA polymerases.

■ ASSOCIATED CONTENT

Supporting Information. Chemical shifts of nonexchangeable protons for the 1,N^2-εdG·dA duplex and exchangeable protons for the 1,N^2-εdG·dA duplex. This material is available free of charge via the Internet at http://pubs.acs.org.

■ AUTHOR INFORMATION

Corresponding Author

*Tel: (615) 322-2589. Fax: (615) 322-7591. E-mail: michael.p.stone@vanderbilt.edu.

Funding Sources

This work was supported by NIH grants P01 ES05355 (C.J.R., I.D.K., and M.P.S.) and R01 ES010375 (F.P.G.). Funding for the NMR spectrometers was supplied by Vanderbilt University, the Vanderbilt Center in Molecular Toxicology, P30 ES00267, and by NIH grant RR005805. The Vanderbilt Ingram Cancer Center is supported by NIH grant P30 CA068485.

■ ABBREVIATIONS

1,N^2-εdG, 3-(2-deoxy-β-D-*erythro*-pentofuranosyl)-3,4-dihydro-9*H*-imidazo[1,2-*a*]purin-9-one or 1,N^2-etheno-2′-deoxyguanosine; PdG, 1,N^2-propano-2′-deoxyguanosine; NOE, nuclear Overhauser enhancement; NOESY, two-dimensional NOE spectroscopy; COSY, correlation spectroscopy; ppm, parts per million; TPPI, time

proportional phase increment. A right superscript refers to numerical position in the sequence starting from the 5′-terminus of chain A and proceeding to the 3′-terminus of chain A and then from the 5′-terminus of chain B to the 3′-terminus of chain B.

REFERENCES

(1) Barbin, A. (2000) Etheno-adduct-forming chemicals: From mutagenicity testing to tumor mutation spectra. *Mutat. Res. 462*, 55–69.

(2) Barbin, A., Bresil, H., Croisy, A., Jacquignon, P., Malaveille, C., Montesano, R., and Bartsch, H. (1975) Liver-microsome-mediated formation of alkylating agents from vinyl bromide and vinyl chloride. *Biochem. Biophys. Res. Commun. 67*, 596–603.

(3) Green, T., and Hathway, D. E. (1978) Interactions of vinyl chloride with rat-liver DNA *in vivo*. *Chem.-Biol. Interact. 22*, 211–224.

(4) Eberle, G., Barbin, A., Laib, R. J., Ciroussel, F., Thomale, J., Bartsch, H., and Rajewsky, M. F. (1989) 1,N^6-etheno-2′-deoxyadenosine and 3,N^4-etheno-2′-deoxycytidine detected by monoclonal antibodies in lung and liver DNA of rats exposed to vinyl chloride. *Carcinogenesis 10*, 209–212.

(5) Fedtke, N., Boucheron, J. A., Walker, V. E., and Swenberg, J. A. (1990) Vinyl chloride-induced DNA adducts. II: Formation and persistence of 7-(2′-oxoethyl)guanine and N^2,3-ethenoguanine in rat tissue DNA. *Carcinogenesis 11*, 1287–1292.

(6) Guengerich, F. P., Mason, P. S., Stott, W. T., Fox, T. R., and Watanabe, P. G. (1981) Roles of 2-haloethylene oxides and 2-haloacetaldehydes derived from vinyl bromide and vinyl chloride in irreversible binding to protein and DNA. *Cancer Res. 41*, 4391–4398.

(7) Guengerich, F. P., and Kim, D. H. (1991) Enzymatic oxidation of ethyl carbamate to vinyl carbamate and its role as an intermediate in the formation of 1,N^6-ethenoadenosine. *Chem. Res. Toxicol. 4*, 413–421.

(8) Guengerich, F. P. (1992) Roles of the vinyl chloride oxidation products 1-chlorooxirane and 2-chloroacetaldehyde in the *in vitro* formation of etheno adducts of nucleic acid bases. *Chem. Res. Toxicol. 5*, 2–5.

(9) Bartsch, H., Barbin, A., Marion, M. J., Nair, J., and Guichard, Y. (1994) Formation, detection, and role in carcinogenesis of ethenobases in DNA. *Drug. Metab. Rev. 26*, 349–371.

(10) Nair, U., Bartsch, H., and Nair, J. (2007) Lipid peroxidation-induced DNA damage in cancer-prone inflammatory diseases: A review of published adduct types and levels in humans. *Free Radical Biol. Med. 43*, 1109–1120.

(11) Lee, S. H., Oe, T., and Blair, I. A. (2002) 4,5-Epoxy-2(*E*)-decenal-induced formation of 1,N^6-etheno-2′-deoxyadenosine and 1,N^2-etheno-2′-deoxyguanosine adducts. *Chem. Res. Toxicol. 15*, 300–304.

(12) Petrova, K. V., Jalluri, R. S., Kozekov, I. D., and Rizzo, C. J. (2007) Mechanism of 1,N^2-etheno-2′-deoxyguanosine formation from epoxyaldehydes. *Chem. Res. Toxicol. 20*, 1685–1692.

(13) Lee, S. H., Arora, J. A., Oe, T., and Blair, I. A. (2005) 4-Hydroperoxy-2-nonenal-induced formation of 1,N^2-etheno-2′-deoxyguanosine adducts. *Chem. Res. Toxicol. 18*, 780–786.

(14) Lee, S. H., and Blair, I. A. (2000) Characterization of 4-oxo-2-nonenal as a novel product of lipid peroxidation. *Chem. Res. Toxicol. 13*, 698–702.

(15) Kawai, Y., Uchida, K., and Osawa, T. (2004) 2′-Deoxycytidine in free nucleosides and double-stranded DNA as the major target of lipid peroxidation products. *Free Radical Biol. Med. 36*, 529–541.

(16) Maekawa, M., Kawai, K., Takahashi, Y., Nakamura, H., Watanabe, T., Sawa, R., Hachisuka, K., and Kasai, H. (2006) Identification of 4-oxo-2-hexenal and other direct mutagens formed in model lipid peroxidation reactions as dGuo adducts. *Chem. Res. Toxicol. 19*, 130–138.

(17) Lee, S. H., Silva Elipe, M. V., Arora, J. S., and Blair, I. A. (2005) Dioxododecenoic acid: A lipid hydroperoxide-derived bifunctional electrophile responsible for etheno DNA adduct formation. *Chem. Res. Toxicol. 18*, 566–578.

(18) Sattsangi, P. D., Leonard, N. J., and Frihart, C. R. (1977) 1,N^2-Ethenoguanine and N^2,3-ethenoguanine synthesis and comparison of electronic spectral properties of these linear and angular triheterocycles related to Y bases. *J. Org. Chem. 42*, 3292–3296.

(19) Guengerich, F. P., Persmark, M., and Humphreys, W. G. (1993) Formation of 1,N^2- and N^2,3-ethenoguanine derivatives from 2-halooxiranes: Isotopic labeling studies and formation of a hemiaminal derivative of N^2-(2-oxoethyl)guanine. *Chem. Res. Toxicol. 6*, 635–648.

(20) Guengerich, F. P., and Persmark, M. (1994) Mechanism of formation of ethenoguanine adducts from 2-haloacetaldehydes: ^{13}C-Labeling patterns with 2-bromoacetaldehyde. *Chem. Res. Toxicol. 7*, 205–208.

(21) Morinello, E. J., Ham, A. J., Ranasinghe, A., Sangaiah, R., and Swenberg, J. A. (2001) Simultaneous quantitation of N^2,3-ethenoguanine and 1,N^2-ethenoguanine with an immunoaffinity/gas chromatography/high-resolution mass spectrometry assay. *Chem. Res. Toxicol. 14*, 327–334.

(22) Marques, S. A., Loureiro, A. P., Gomes, O. F., Garcia, C. C., Di Mascio, P., and Medeiros, M. H. (2004) Induction of 1,N^2-etheno-2′-deoxyguanosine in DNA exposed to beta-carotene oxidation products. *FEBS Lett. 560*, 125–130.

(23) Kawai, Y., Kato, Y., Nakae, D., Kusuoka, O., Konishi, Y., Uchida, K., and Osawa, T. (2002) Immunohistochemical detection of a substituted 1,N^2-ethenodeoxyguanosine adduct by omega-6 polyunsaturated fatty acid hydroperoxides in the liver of rats fed a choline-deficient, L-amino acid-defined diet. *Carcinogenesis 23*, 485–489.

(24) Loureiro, A. P., Marques, S. A., Garcia, C. C., Di Mascio, P., and Medeiros, M. H. (2002) Development of an on-line liquid chromatography-electrospray tandem mass spectrometry assay to quantitatively determine 1,N^2-etheno-2′-deoxyguanosine in DNA. *Chem. Res. Toxicol. 15*, 1302–1308.

(25) Martinez, G. R., Loureiro, A. P., Marques, S. A., Miyamoto, S., Yamaguchi, L. F., Onuki, J., Almeida, E. A., Garcia, C. C., Barbosa, L. F., Medeiros, M. H., and Di Mascio, P. (2003) Oxidative and alkylating damage in DNA. *Mutat. Res. 544*, 115–127.

(26) Pang, B., Zhou, X., Yu, H., Dong, M., Taghizadeh, K., Wishnok, J. S., Tannenbaum, S. R., and Dedon, P. C. (2007) Lipid peroxidation dominates the chemistry of DNA adduct formation in a mouse model of inflammation. *Carcinogenesis 28*, 1807–1813.

(27) Medeiros, M. H. (2009) Exocyclic DNA adducts as biomarkers of lipid oxidation and predictors of disease. Challenges in developing sensitive and specific methods for clinical studies. *Chem. Res. Toxicol. 22*, 419–425.

(28) Langouet, S., Mican, A. N., Muller, M., Fink, S. P., Marnett, L. J., Muhle, S. A., and Guengerich, F. P. (1998) Misincorporation of nucleotides opposite five-membered exocyclic ring guanine derivatives by *Escherichia coli* polymerases *in vitro* and *in vivo*: 1,N^2-Ethenoguanine, 5,6,7,9-tetrahydro-9-oxoimidazo[1,2-*a*]purine, and 5,6,7,9-tetrahydro-7-hydroxy-9-oxoimidazo[1,2-*a*]purine [published erratum appears in Biochemistry 1998 Jun 16;37(24):8816]. *Biochemistry 37*, 5184–5193.

(29) Akasaka, S., and Guengerich, F. P. (1999) Mutagenicity of site-specifically located 1,N^2-ethenoguanine in Chinese hamster ovary cell chromosomal DNA. *Chem. Res. Toxicol. 12*, 501–507.

(30) Zang, H., Goodenough, A. K., Choi, J. Y., Irimia, A., Loukachevitch, L. V., Kozekov, I. D., Angel, K. C., Rizzo, C. J., Egli, M., and Guengerich, F. P. (2005) DNA adduct bypass polymerization by *Sulfolobus solfataricus* DNA polymerase Dpo4: Analysis and crystal structures of multiple base pair substitution and frameshift products with the adduct 1,N^2-ethenoguanine. *J. Biol. Chem. 280*, 29750–29764.

(31) Ling, H., Boudsocq, F., Woodgate, R., and Yang, W. (2001) Crystal structure of a Y-family DNA polymerase in action: A mechanism for error-prone and lesion-bypass replication. *Cell 107*, 91–102.

(32) Zaliznyak, T., Lukin, M., Johnson, F., and de Los Santos, C. (2008) Solution structure of duplex DNA containing the mutagenic lesion 1,N^2-etheno-2′-deoxyguanine. *Biochemistry* 4606–4613.

(33) Shanmugam, G., Kozekov, I. D., Guengerich, F. P., Rizzo, C. J., and Stone, M. P. (2008) Structure of the 1,N^2-ethenodeoxyguanosine adduct opposite cytosine in duplex DNA: Hoogsteen base pairing at pH 5.2. *Chem. Res. Toxicol. 21*, 1795–1805.

(34) Shanmugam, G., Goodenough, A. K., Kozekov, I. D., Guengerich, F. P., Rizzo, C. J., and Stone, M. P. (2007) Structure

of the 1,N^2-etheno-2′-deoxyguanosine adduct in duplex DNA at pH 8.6. *Chem. Res. Toxicol. 20*, 1601–1611.

(35) Goodenough, A. K., Kozekov, I. D., Zang, H., Choi, J. Y., Guengerich, F. P., Harris, T. M., and Rizzo, C. J. (2005) Site specific synthesis and polymerase bypass of oligonucleotides containing a 6-hydroxy-3,5,6,7-tetrahydro-9H-imidazo[1,2-*a*]purin-9-one base, an intermediate in the formation of 1,N^2-etheno-2′-deoxyguanosine. *Chem. Res. Toxicol. 18*, 1701–1714.

(36) Cavaluzzi, M. J., and Borer, P. N. (2004) Revised UV extinction coefficients for nucleoside-5′-monophosphates and unpaired DNA and RNA. *Nucleic Acids Res. 32*, e13.

(37) Piotto, M., Saudek, V., and Sklenar, V. (1992) Gradient-tailored excitation for single-quantum NMR spectroscopy of aqueous solutions. *J. Biomol. NMR 2*, 661–665.

(38) Reid, B. R. (1987) Sequence-specific assignments and their use in NMR studies of DNA structure. *Q. Rev. Biophys. 20*, 2–28.

(39) Patel, D. J., Shapiro, L., and Hare, D. (1987) DNA and RNA: NMR studies of conformations and dynamics in solution. *Q. Rev. Biophys. 20*, 35–112.

(40) Boelens, R., Scheek, R. M., Dijkstra, K., and Kaptein, R. (1985) Sequential assignment of imino- and amino-proton resonances in ^{1}H NMR spectra of oligonucleotides by two-dimensional NMR spectroscopy. Application to a *lac* operator fragment. *J. Magn. Reson. 62*, 378–386.

(41) Choi, J. Y., Chowdhury, G., Zang, H., Angel, K. C., Vu, C. C., Peterson, L. A., and Guengerich, F. P. (2006) Translesion synthesis across O^6-alkylguanine DNA adducts by recombinant human DNA polymerases. *J. Biol. Chem. 281*, 38244–38256.

(42) Langouet, S., Muller, M., and Guengerich, F. P. (1997) Misincorporation of dNTPs opposite 1,N^2-ethenoguanine and 5,6,7,9-tetrahydro-7-hydroxy-9-oxoimidazo[1,2-*a*]purine in oligonucleotides by *Escherichia coli* polymerases I *exo-* and II *exo-*, T7 polymerase *exo-*, human immunodeficiency virus-1 reverse transcriptase, and rat polymerase beta. *Biochemistry 36*, 6069–6079.

(43) Singh, U. S., Moe, J. G., Reddy, G. R., Weisenseel, J. P., Marnett, L. J., and Stone, M. P. (1993) ^{1}H NMR of an oligodeoxynucleotide containing a propanodeoxyguanosine adduct positioned in a $(CG)_3$ frameshift hotspot of *Salmonella typhimurium hisD3052*: Hoogsteen base-pairing at pH 5.8. *Chem. Res. Toxicol. 6*, 825–836.

(44) Huang, H., Wang, H., Lloyd, R. S., Rizzo, C. J., and Stone, M. P. (2009) Conformational interconversion of the trans-4-hydroxynonenal-derived (6*S*,8*R*,11*S*) 1,N^2-deoxyguanosine adduct when mismatched with deoxyadenosine in DNA. *Chem. Res. Toxicol. 22*, 187–200.

(45) Kouchakdjian, M., Marinelli, E., Gao, X., Johnson, F., Grollman, A., and Patel, D. (1989) NMR studies of exocyclic 1,N^2-propanodeoxyguanosine adducts (X) opposite purines in DNA duplexes: Protonated X(*syn*):A(*anti*) pairing (acidic pH) and X(*syn*):G(*anti*) pairing (neutral pH) at the lesion site. *Biochemistry 28*, 5647–5657.

(46) Kouchakdjian, M., Eisenberg, M., Live, D., Marinelli, E., Grollman, A. P., and Patel, D. J. (1990) NMR studies of an exocyclic 1,N^2-propanodeoxyguanosine adduct (X) located opposite deoxyadenosine (A) in DNA duplexes at basic pH: Simultaneous partial intercalation of X and A between stacked bases. *Biochemistry 29*, 4456–4465.

(47) Shanmugam, G., Kozekov, I. D., Guengerich, F. P., Rizzo, C. J., and Stone, M. P. (2010) Structure of the 1,N^2-etheno-2′-deoxyguanosine lesion in the 3′-G(εdG)T-5′ sequence opposite a one-base deletion. *Biochemistry 49*, 2615–2626.